e-Polymers **2009**, no. 054

http://www.e-polymers.org

ISSN 1618-7229

The role of the matrix-filler affinity on morphology and properties of polyethylene/clay and polyethylene/ compatibilizer/clay nanocomposites drawn fibers

Nadka Tzankova Dintcheva,[*] *Rosamaria Marino, Francesco Paolo La Mantia*

[*]Dipartimento di Ingegneria Chimica dei Processi e dei Materiali, Università di Palermo, Viale delle Scienze, ed. 6, 90128 Palermo, Italy; fax: +390916567280; tel: +390916567204; e-mail: dintcheva@dicpm.unipa.it, r.marino@dicpm.unipa.it, lamantia@dicpm.unipa.it

(Received: 22 December, 2007; published: 31 May, 2009)

Abstract: In this work the structural variations and mechanical performance of polyethylene/clay nanocomposite drawn fibres, also in the presence of compatibilizer, such as a commercial maleic anhydride grafted polyethylene, PEgMA, was studied. In the isotropic state both systems show intercalated morphology.

After spinning and cold drawing, by adding the nanoparticles, the tensile strength as a function of the draw ratio increases and this rise is more pronounced for the filled compatibilized system. The reduction of the elongation at break, on the contrary, is about the same for all the examined samples. The orientation of the macromolecules, evaluated by measurements of the birefringence and calorimetric analysis, is similar for all the samples, but the filled, drawn fibres show a higher level of intercalation and, in particular, some exfoliation, more and more pronounced with the draw ratio and in presence of compatibilizer, as a consequence of the application of the extensional (at low and high temperature) flow. For the three components system with greater affinity between the polymer matrix and clay, the extensional flow is more efficient. The initial intercalated morphology changes to some more intercalation and finally, at the highest anisotropic condition in the presence of the PEgMA, evolves to delaminated clay structure.

Keywords: nanocomposite polyolefin fibre; extensional flow; matrix-filler affinity.

Introduction

The morphology and material properties of polymer/clay nanocomposites depend on the type of the matrix, on the affinity between clay and polymer, on the processing conditions, on the type and amount of filler, and on the formation of intercalated, exfoliated or hybrid clay dispersion [1-4]. Some works affirm that the presence of the small amount of a polar polymer, as maleic anhydride grafted polyethylene, is able to change the properties of the polyolefin nanocomposites [5-8]. In particular, an increased tenacity of polyolefin/compatibilizer/clay fibres is obtained as a function of the nano-filler content and of the draw ratio as a result of some exfoliation. Zhang [8] et al. reported that the significant increased interaction between polyethylene matrix and filler in the presence of maleic anhydride grafted polyethylene is responsible for the distinct improvement in mechanical properties of these nanocomposite systems.

The morphology of incompatible blends is strongly dependent on the type of flow; even if the viscosity of the two phases is considerably different [9-10], the applied

elongational flow is able to break-up, disperse and orientate the particles of the dispersed system. This does not occur in shear flow.

In previous our work [11], we studied the effect of the elongational flow induced morphology on the polyethylene-clay nanocomposites. In presence of limited affinity between polyethylene and organoclay, the applied elongational flow gives rise to exfoliation of intercalated tactoids and to some more intercalation of the same tactoids and consequently the mechanical properties strongly increases more than that of the pure polyethylene.

In this work a commercial maleic anhydride grafted polyethylene was used to change the affinity between the polymer and organoclay in order to demonstrate that the elongation flow induced exfoliation is more efficient with increasing the affinity between the two phases. The morphology and the properties of polyethylene/clay nanocomposites drawn fibres have been compared with those of the fibres with the same composition but in presence of maleic anhydryde grafted polyethylene.

Results and discussion

Tensile strength, TS and elongation at break, EB, values for all the samples at different draw ratio are reported in Table 1. The draw ratio, DRc, is the ratio applied during the cold-drawing, DRc = 0 corresponds to the compression moulded samples, while DRc = 1 represents the spun fibres. In the isotropic state (DRc = 0), the presence of a small amount of functionalized polyethylene does not cause any significant change of the mechanical properties with respect to the pure (filled or unfilled) polymer. With increasing the draw ratio for all the samples, in particular in the highly anisotropic conditions, a significant rise of the tensile strength and a contemporary reduction of the elongation at break are observed. By adding the compatibilizer, the increase of the mechanical properties is higher than that shown by the uncompatibilized samples.

Tab. 1. Mechanical properties of all the samples at different draw ratio.

DRc	PE		PE/CL		PE/PEgMA		PE/PEgMA/CL	
	TS, MPa	EB, %	TS, MPa	EB, %	TS, MPa	EB, %	TS, MPa	EB, %
0	27	722	25	715	25	753	24	733
1	47	626	64	656	52	602	80	670
3	135	220	209	240	200	211	259	199
4	169	127	275	130	266	120	347	127
5	192	82	327	90	314	102	394	95
6	280	48	500	60	463	59	591	60

To better observe this last phenomenon, the dimensionless mechanical properties of all the samples as a function of the draw ratio are reported in Figs. 1-2.

The dimensionless values have been calculated by dividing the values relative to the fibres by those of the compression moulded sheets (DRc=0). As previously observed, by adding the nanoparticles the increase of the dimensionless tensile strength as a function of the draw ratio is more pronounced for system PE/PEgMA/CL. On the contrary, the reduction of the elongation at break with drawing is about the same for the four investigated samples. The presence of PEgMA improves the affinity between

the matrix and the nanoparticles and can be considered as responsible for this behavior, as confirmed later on by morphological analysis.

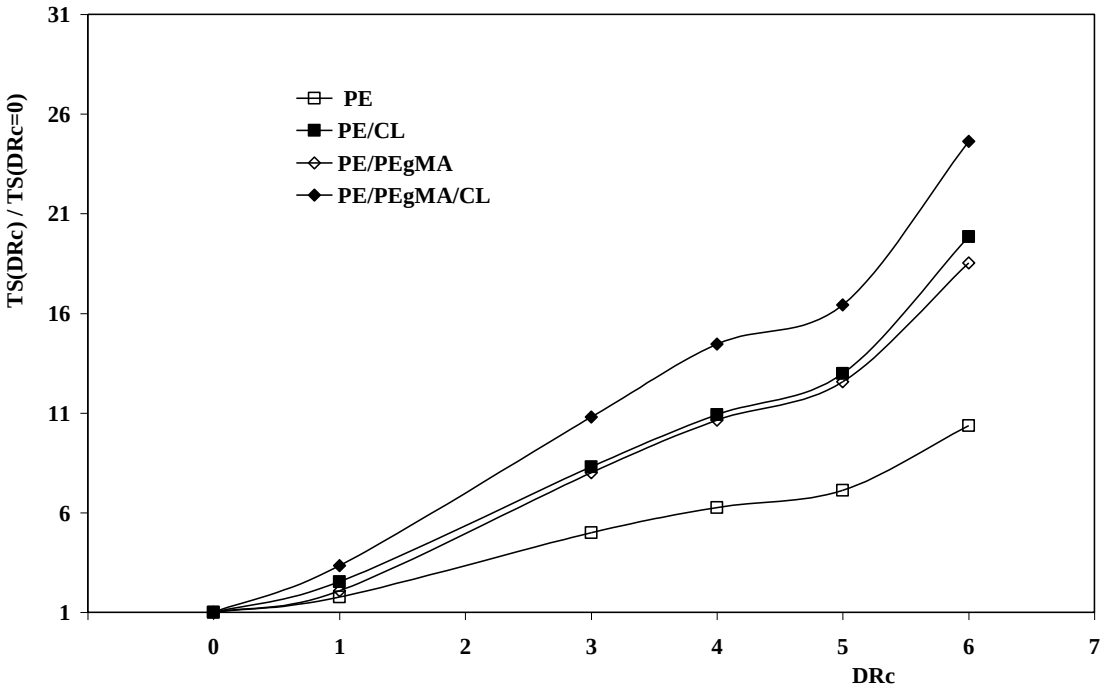

Fig. 1. Dimensionless tensile strength of all samples as a function of the draw ratio.

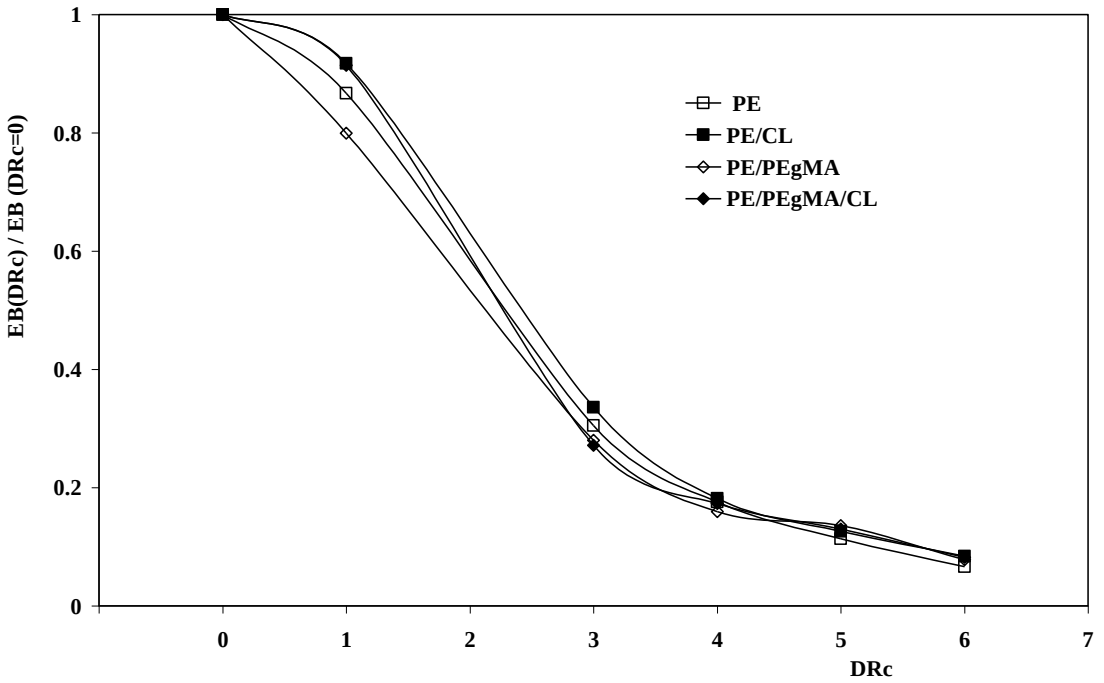

Fig. 2. Dimensionless elongation at break of all samples as a function of the draw ratio.

In a previous paper [11], the same level of orientation of the macromolecules, achieved both during the melt spinning and the cold drawing, was evaluated for both filled and unfilled samples and the better improvement of the mechanical properties was attributed to the partial exfoliation of the nanoparticles induced by the elongational flow. Following the same procedure, the total birefringence and calorimetric analysis were performed on all the investigated samples and the results are reported in the Table 2. All these data and eq. 1, suggest that the orientation of the crystalline and amorphous phases for all the samples are similar. The different increase of the mechanical properties of the filled, compatibilized samples cannot then be attributed to some different chain orientation but could be attributed to the formation of different morphologies.

Tab. 2. Crystalline degree and total birefringence of as spun and drawn (DRc=6) PE/CL and PE/PEgMA/CL fibres.

Samples	Crystalline degree, %	Total birefringence * 10-3
As spun fibre		
PE fibre	43.4	4.1
PE/CL fibre	42.2	4.5
PE/PEgMA fibre	41.2	4.2
PE/PEgMA/CL fibre	40.5	4.5
Drawn fibre		
PE DRc=6	45.5	12.1
PE/CL DRc=6	44.5	12.6
PE/PEgMA DRc=6	42.8	12.0
PE/PEgMA/CL DRc=6	42.0	12.5

In this previous work [11], we proposed to consider the behaviour during drawing of polyethylene-clay nanocomposites like that of polymer blends. The dispersed clay nanoparticles can be broken and oriented (along the flow direction) by the extensional flow. The morphology of the clay particles, under the applied elongational flow, changes from intercalated to hybrid (intercalated and exfoliated) structures, and the presence of some more intercalated tactoids are also observed.

By adding the compatibilizer, the morphology of the polyethylene/clay nanocomposites is different as a better adhesion between matrix and clay particles is expected. In order to evaluate the morphology of the two systems with different affinity - polyethyelene/clay and polyethylene/compatibilizer/clay systems - WAXS and TEM analysis were performed. The WAXS traces and the interlayer distance and number of platelets per stack of compounded, as spun and drawn PE/CL and PE/PEgMA/CL fibres are reported in Fig. 3 and Tab. 3 respectively.

The x-ray traces of both compounded anisotropic samples clearly show intercalated morphology. The interlayer distances of PE/CL and PE/PEgMA/CL samples after the copmpounding are 3.30 and 3.42 nm, respectively. These values of the interlayer distances are higher than that the pristine Cloisite 15A, see Tab. 3. Indeed, the reduction of the number of platelets/stack for the uncompatibilized sample is observed, and this reduction is more pronounced in the presence of the PEgMA, confirming more intercalation in the presence of the compatibilizer.

The TEM micrographs of the two isotropic systems, confirm the different intercalation, see Fig. 4 (a) and (d). The surface area of the clay particles is then

different for the two systems with different affinity, even if the interlayer distance, evaluated by x-ray analyses, is slightly changed.

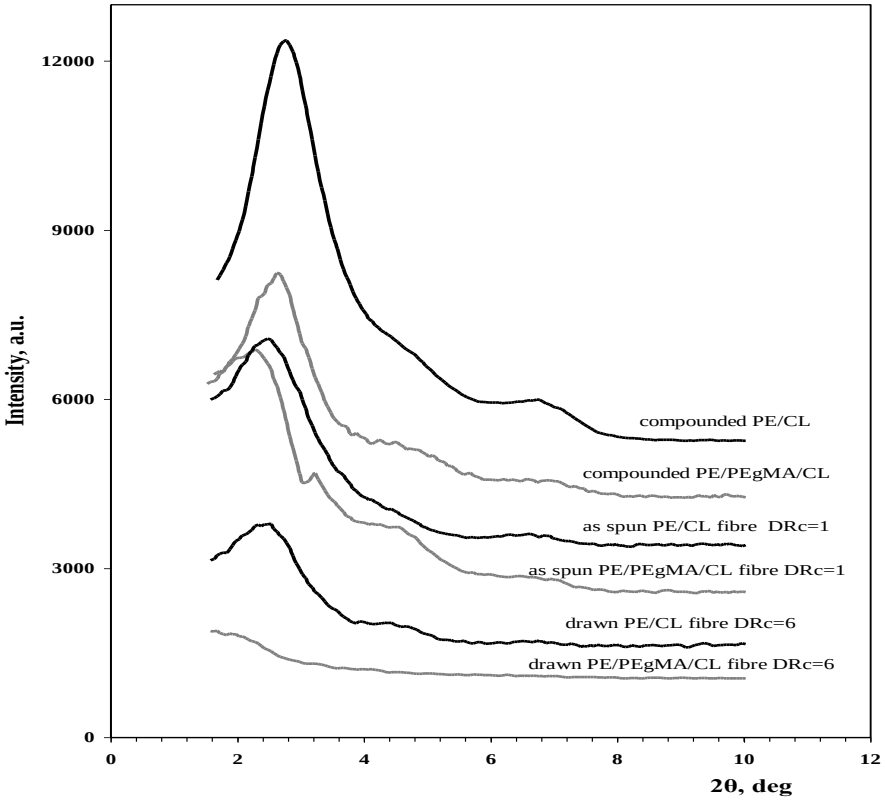

Fig. 3. WAXS traces of compounded, as spun and drawn fibre (DRc=6) PE/CL - black traces - and of compounded, as spun and drawn fibre (DRc=6) PE/PEgMA/CL - grey traces.

Tab. 3. Main x-ray peak, interlayer distance and number of platelets per stack of compounded, as spun and drawn (DRc=6) PE/CL and PE/PEgMA/CL fibres and of the pristine Cloisite.

Samples	Main peak 2θ, deg	Interlayer distance d_{001}, nm	Platelets/stack, N
CL 15A	2.80	3.15	3.11
compounded PE/CL	2.67	3.30	2.61
as spun PE/CL fibre	2.53	3.48	2.15
drawn PE/CL fibreb DRc=6	2.32	3.81	2.02
compounded PE/PEgMA/CL	2.58	3.42	2.33
as spun PE/PEgMA/CL fibre	2.16	4.09	2.08
drawn PE/PEgMA/CL fibre DRc=6	---	---	---

The different affinity between the polymer and clay determines then slightly different initial morphologies before the application of the extensional flow. By applying the extensional flow, different evolutions of the clay morphology are observed.

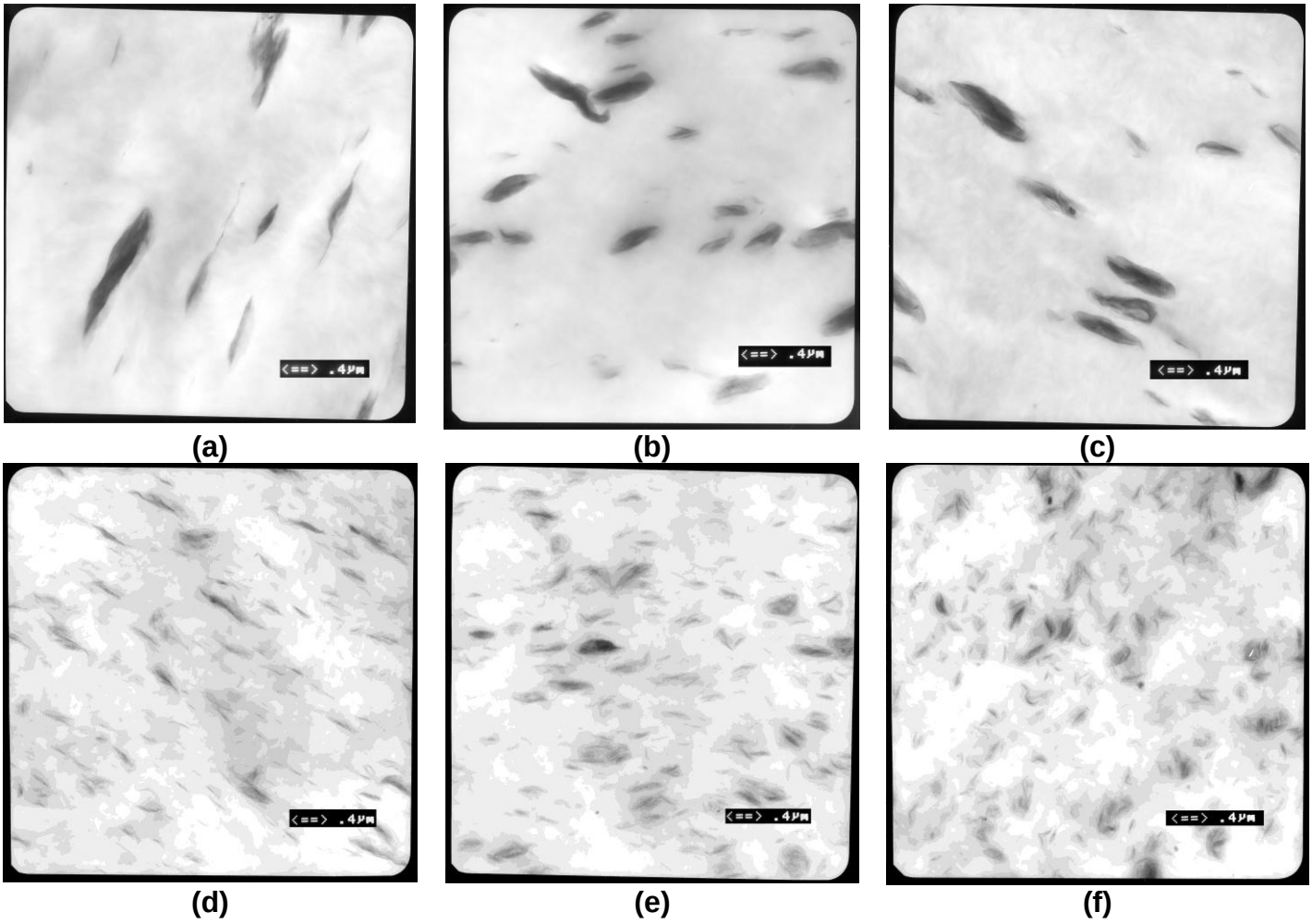

Fig. 4. TEM micrographs of (a) compounded, (b) as spun fibre and (c) drawn fibre (DRc=6) PE/CL and (d) compounded, (e) as spun fibre and (f) drawn fibre (DRc=6) PE/PEgMA/CL at different magnifications.

Indeed, the X-ray traces of the as spun fibre and drawn fibres of the two systems are plotted in Fig. 3, put in evidence a change from intercalated to hybrid (co-existence of intercalated and exfoliated) clay morphology. With increasing the draw ratio for both systems the interlayer distances increase and the number of platelets/stack decrease, see Table 3. In particular, at the highest anisotropic conditions (DRc=6) and in the presence of the compatibilizer, no peak is observed. The TEM micrograph of PE/PEgMA/CL sample, reported in Fig. 4 (f), shows well dispersed, delaminated and regular nanoparticles.

The above morphological analyses suggest that the application of the cold draw causes the exfoliation of intercalated tactoids and some more intercalation of the same tactoids for both systems, but in particular for the PE/PEgMA/CL system with greater affinity between the polymer matrix and clay. The presence of the compatibilizer and the consequent better affinity between matrix and clay makes the

extensional flow more efficient even if it does not seem a necessary condition to provoke the exfoliation of the intercalated tactoids [11].

The distribution curves of the area (surface) dimensions of the nanoparticles in all samples were evaluated and plotted in Figure 5. For compounded PE/CL, as spun fibre and drawn fibres, with increasing the draw ratio, the peaks of curves of the nanoparticles shift towards lower values and the height of the main peaks decrease.

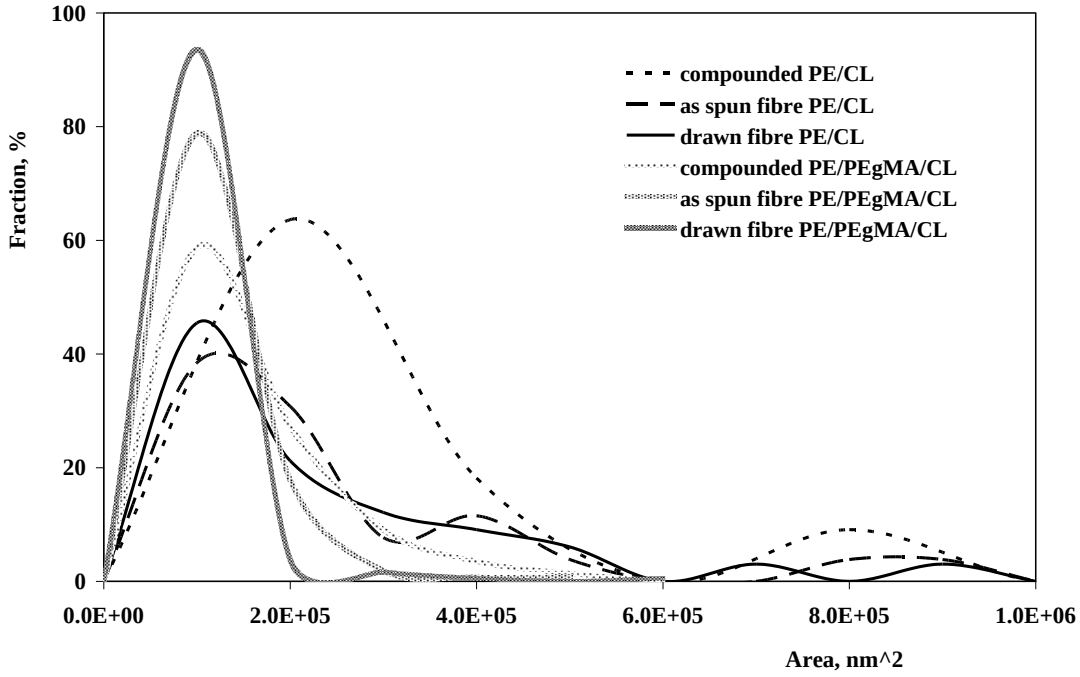

Fig. 5. Distribution curves of the areas of the nanoparticles for three PE/CL samples and for three PE/PEgMA/CL samples: compounded, as spun and drawn fibre (DRc = 6) respectively.

Indeed, a multi-modular distribution curve with increasing of the draw ratio is observed. These curves have been interpreted [11] as an increase of the number of exfoliated particles or of clay particles with a lower number of platelets, in agreement with the calculated number of platelets/stack, reported in Table 3. As for the compatibilized system, no multi-modular distribution curve is observed and this is easily interpreted with the more homogenous exfoliated morphology. Going from isotropic to anisotropic conditions for PE/PEgMA/CL samples, the distribution curves of the area of the nanoparticles slowly shift towards lower values, but the height of the single peak increases. In particular, at the highest anisotropic conditions, the observed peak suggests that about 90 % of the nanoparticles show a surface between 0 and $2*10^5$ nm^2. The fraction of the nanoparticles with surface greater than $2*10^5$ nm^2 disappears. In agreement with the disappeared x-ray peak and TEM micrographs, reported in Fig. 4 (f), these data suggest the presence of nanoparticles with more regular and homogenous exfoliated morphology.

Conclusions

The mechanical performance and variations of the clay morphology of polyethylene/clay nanocomposite drawn fibre, also in the presence of a PEgMA, able

to change significantly the affinity between the matrix and clay, were studied. Significant increase of the tensile strength is observed in the presence of small amount of the organo-modified nanoparticles (at 5% wt/wt.) as a function of the extensional flow. In particular, this increase is slightly more pronounced for the system with improved affinity between the matrix and filler and especially with respect to the isotropic sample. Some reduction of the elongation at break for all investigated systems, in particular, at high anisotropic conditions, is observed. The calorimetric analyses and measurement of the total birefringence of all the systems indicate about the same orientation of the macromolecules achieved by applied extensional flow.

The morphological analyses for the system with reduced affinity between matrix and nanoparticles, suggest the exfoliation of intercalated tactoids and some more intercalation of same tactoids occurs as a consequence of the cold drawing the system with greater affinity, in particular at the highest anisotropic conditions it shows an almost compact delaminated clay structure.

The improvement of the material properties of polyethylene/compatibilizer/clay system is due to both improved affinity and more uniform exfoliated clay particles.

Acknowledgments

The work has been financially supported by University of Palermo, RS. 2007.

Thanks are due to Prof. P.L. Magagnini (University of Pisa) for the WAXS spectra and to Dr. G. Costa (ISMac – C.N.R. Genova) for the TEM micrographs and for the valuable discussions. When this manuscript was submitted, Giovanna Costa – a smart and honest researcher as well as a very good friend of ours, unexpectedly died.

Experimental part

Materials

The materials used in this work were a sample of film-grade polyethylene, a linear low density polyethylene e sample, PE, (Clearflex FG166, M_w = 130,000 g mol^{-1}, M_w/M_n = 3.8, $MFI_{190°C/2.16kg}$ = 0.27 g 10 min^{-1} and ρ = 0.918 g cm^{-3} at room temperature; from Polimeri Europa, Italy) and an organo-modified clay sample (Cloisite® 15A, from Southern Clay Products). Cloisite 15A, CL, is a dimethyl dihydrogenated tallow quaternary ammonium modified montmorillonite with an average diameter of 8 μm; the organo-modifier concentration is 125 meq / 100 g clay. As a compatibilizer was used a sample of maleic anhydride grafted polyethylene, PEgMA, with 1 wt% MA and $MFI_{190°C/2.16kg}$ = 5 g10 min^{1} (Polybond 3009, from Crompton Corp.).

Processing and characterization

LLDPE has been compounded with 5 % wt/wt of organoclay in a corotating intermeshing twin screw extruder (OMC, Italy; D = 19 mm, L/D = 35) with thermal profile: 120-140-150-160-170-180 °C and mixing speed: 220 rpm. The compatibilized samples were prepared in the same conditions and by adding 5% wt/wt of PEgMA. For comparison, the pure polymer was subjected to the same extrusion process. The residence time was about 90-110 s.

The fibres were spun by using a capillary viscometer (Rheoscope 1000, CEAST, Italy) operating under a constant extrusion speed (5 mm/min), with a die of 1 mm diameter (D_0) at 180 °C. The filaments were extruded in air at room temperature. The take-up velocity was about 4 m/min. The final diameter of the as spun fibres, D_f, was about 0.2 mm and draw ratio about 25.

The spun fibres were drawn with the aid of an Instron machine (mod. 1122) at room temperature and at a crosshead speed of 100 mm/min. The initial length was in all the cases 50 mm. The amount of drawing is characterized by the draw ratio (DRc = L_f/L_0) where L_f is the final length and L_0 the initial length of the fibres.

Mechanical tests were carried out with the same universal Instron machine used for the cold drawing and according to ASTM D882. Average values for tensile strength (TS) and elongation at break (EB) were obtained by analyzing the results of ten tests per samples. The reproducibility of the results was about ± 5% from the average. The mechanical behavior of the fibres was compared with that of rectangular samples cut from compression molded sheet, prepared at 180 °C. The thickness of the sheet was about 60 μm.

WAXD patterns were obtained by a Siemens D-500 diffractometer in the reflection mode with an incident X-ray wavelength of 0.1542 nm. The interlayer distance and the number of clay per average stack were calculated as reported in [12].

TEM observations were made with a ZEISS EM 900 microscope, at accelerating voltages of 50 and 80 KeV, in the Genoa division of the Institute for Macromolecular Studies (ISMac) of C.N.R. Samples for TEM analysis were taken either from pieces of the compounded nanocomposites and from the fibres at different DRc. The analyses were carried out on the radial surface for both extruded and fibre samples. Image analysis was carried out by using Q-win Leica software. For each samples, the distribution of the dimensions of the particles of the dispersed phase, by evaluating the area, was determined and reported.

The calorimetric data were evaluated by differential scanning calorimetry, using a Perkin-Elmer DSC7, at scanning rate of 20 °C/min.

All the birefringence measurements were performed at room temperature using a Leitz polarizing microscope equipped with a Berek compensator. The total birefringence is a function of the crystalline and amorphous birefringence according to the following equation:

$$\Delta n = \Delta n_c f_c x_c + \Delta n_a f_a (1-x_c) + \Delta n_f \quad (1)$$

where Δn_c, Δn_a and f_c, f_a are the intrinsic values of the birefringence and the orientation factors of the crystalline and amorphous phase, respectively, and x_c is the crystalline degree. The form birefringence, Δn_f, is usually considered negligible with respect to the other terms.

References

[1] Alexandre, M.; Dubois, P. *Mat. Sci. Eng.,* **2000,** *28*, 1.
[2] Krishnamoorti, R.; Ren, J. ; Silva, A. S. *J Chem Phys*, **2001**, *114*, 4968.
[3] Ray, S. S. ; Okamoto, M. *Prog. Polym. Sci.*, **2003**, *28*, 1539.
[4] La Mantia, F.P.; Tzankova Dintcheva, N.; Filippone, G.; Acierno, D. *J. Appl. Polym. Sci*., **2006**, *102*, 4749.

[5] Pavlikova, S.R.; Reichert, T.P.; Mulhaupt, R.; Marcincin, A.; Borsig, E. *J. Appl. Polym. Sci.,* **2003**, *89*, 604.
[6] Mlynarcikova, Z.; Kaempfer, D.; Thomann, R.; Mulhaupt, R.; Borsig, E. *Polym. Adv. Technol.*, **2005**, *16*, 362.
[7] Joshi, M.; Viswnathan, V. *J. Appl. Polym. Sci.*, **2006**, *102*, 2164.
[8] Zhang, M.; Sundararaj, U. *Macromol. Mater. Eng.* **2006**, *291*, 697.
[9] Utracki, L.A. *"*Polymers Alloys and Blends", **1990**, Hanser Publishers, New York.
[10] Lyngaae-Jorgensen, J. "*Rheology of Polymer Blends*" in M.J. Folkes, P.S. Hope eds., "Polymer Blends and Alloys", **1993**, Blackie Academic & Professional, London.
[11] La Mantia, F.P.; Tzankova Dintcheva, N.; Scaffaro, R.; Marino, R. *Macromol. Mater. Eng.* **2008**, *293,* 83.
[12] Tokihisa, M.; Yakemoto, K.; Sakai, T.; Utracki, L.A.; Sepehr, M.; Li, J.; Simard, Y. *Polym. Eng. Sci*., **2006**, *46*, 1040.